Hardware-in-the-Loop Methods for Real-Time Frequency-Response Measurements of on-Board Power Distribution Systems

Tomi Roinila, *Member, IEEE*, Tuomas Messo, *Member, IEEE*, Roni Luhtala, *Student Member, IEEE*, Rick Scharrenberg, Erik C. W. de Jong, *Senior Member, IEEE*, Alejandra Fabian, and Yin Sun

***Abstract*—The operation of more electric aircraft is dependent on the embedded power grid. Therefore, the on-board power-distribution system must be reliable, having a high level of survivability, and promptly respond to any change in aircraft's operation. Recent studies have presented a number of frequency-response-based tools with which to analyze both single- and multiconverter systems. The methods can be efficiently applied for on-board system analysis, stability assessment, and adaptive control design. Most often, wideband measurement techniques have been applied to obtain the frequency response from a specific converter or a subsystem required for the analysis. In the methods, a broadband excitation such as a pseudorandom binary sequence (PRBS) is used as an external injection, and Fourier techniques are applied to extract the spectral information. This paper presents implementation techniques of the wideband methods using power-hardware-in-the-loop measurements based on OPAL-RT real-time simulator. The presented methods make it possible to modify the system characteristics, such as impedance behavior, in real time, thereby providing means for various stability and control design tools for on-board power distribution systems. Experimental measurements are shown from a high-power energy distribution system recently developed at DNV GL, Arnhem, The Netherlands.**

***Index Terms*—Frequency response, hardware-in-the loop simulation, microgrids, power distribution, system identification.**

I. Introduction

EMBEDDED power grids have become popular in more electric aircraft (MEA) [1]. This concept has enabled several advantages in the aircraft industry, such as decrease in weight, increased reliability, reduce in fuel consumption, and passenger comfort. As the requirements of electric load in aircrafts is constantly increasing, maintaining the MEA strongly relies on optimized on-board electrical network and power-electronics conversion systems.

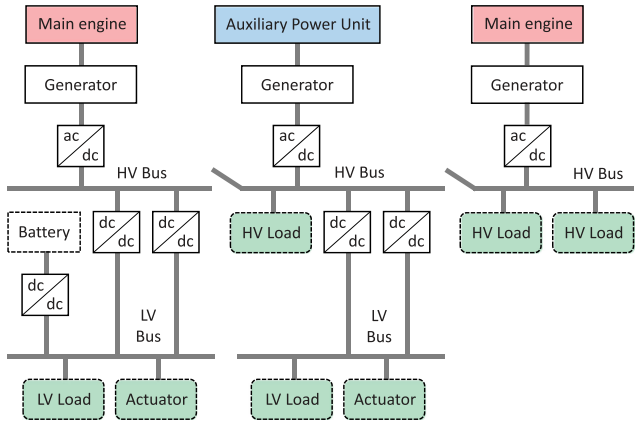

Fig. 1. Simplified power distribution system for aircraft.

Embedded power grids are most often composed by various converters creating a complex interconnected system. Fig. 1 shows a simplified example of a power distribution system for an aircraft [2]. Each of the interconnected converters typically has a high-bandwidth feedback control. Due to interactions among the converter feedback loops through dc bus interconnections, converters that are standalone stable may exhibit different dynamic behavior when interconnected and small-signal stability may be compromised [3]. Because of reduced grid size, the interactions between the converters are often strong, leading to undesirable operation and even to instability [4]. The major challenges of such systems include the power flow regulation, the voltage stability, and the varying dynamic characteristics of the grid [5].

Several stability criteria have been proposed to assess the stability of interconnected power-electronics systems. In the case of grid-connected systems, one of the most utilized techniques has been the impedance-based stability criterion [6]. In the method, the system stability is assessed by the ratio between the systems impedance and converter output impedance. The system will

Manuscript received April 30, 2018; revised June 29, 2018; accepted July 12, 2018. Date of publication August 6, 2018; date of current version February 28, 2019. This work was supported in part by the Academy of Finland and in part by European Union. *(Corresponding author: Tomi Roinila.)*

T. Roinila and R. Luhtala are with the Laboratory of Automation and Hydraulics, Tampere University of Technology, 33720 Tampere, Finland (e-mail: tomi.roinila@tut.fi; roni.luhtala@tut.fi).

T. Messo is with the Laboratory of Electrical Energy Engineering, Tampere University of Technology, 33720 Tampere, Finland (e-mail: tuomas.messo@tut.fi).

R. Scharrenberg, E. C. W. de Jong, A. Fabian, and Y. Sun are with the DNV GL, 6812 AR Arnhem, The Netherlands (e-mail: rick.scharrenberg@dnvgl.com; erik.de.jong@dnvgl.com; alejandra.fabian@dnvgl.com; yin.sun@dnvgl.com).

Color versions of one or more of the figures in this paper are available online at http://ieeexplore.ieee.org.

Digital Object Identifier 10.1109/TIE.2018.2860543

remain stable if the impedance ratio satisfies the Nyquist stability criterion. Impedance-based analysis techniques have also been presented for dc systems in which multiple converters are interconnected through dc bus: the passivity-based stability criterion, and the concept of an allowable impedance region based on the Nyquist contour of the system bus impedance have been utilized [7]. One of the advantages of the impedance-based techniques is that they can be applied based on impedance measurements that do not require *a priori* knowledge of system parameters. These methods are well-suited for online stability assessment and adaptive control tuning [8].

Studies have presented a number of measurement methods suitable for fast, accurate online frequency-response measurement of interconnected power-electronics systems [9]–[14]. Roinila *et al.* in [9] presented an online technique for a grid-impedance measurement. In this method, a pseudorandom binary sequence (PRBS) was injected into a voltage reference of an existing grid-connected three-phase inverter. The resulting responses in the grid voltage and currents were measured, and the grid impedance was computed by Fourier methods. Martin *et al.* in [10] applied similar techniques for measuring ac system impedances. The work in [11] utilized the PRBS for control design and measured the bus impedance from a multiconverter system. This paper was extended in [12], and orthogonal binary sequences were applied for simultaneous measurement of several (coupled) impedances in a multiconverter system. Measurement techniques based on orthogonal injections were also applied in [13], which considered simultaneous measurement of grid-impedance d- and q-components. Nonlinearities involved in power-electronics systems were considered in [14] and a ternary-sequence injection was applied for obtaining impedances from a grid-connected system. The sequence is very similar to the conventional PRBS, but the signal has three levels instead of two. The signal type is particularly useful for systems exhibiting strong nonlinear characteristics.

This paper considers real-time frequency-domain identification and stability analysis of an interconnected power-distribution system using OPAL-RT power-hardware-in-the-loop (PHIL) setup recently developed at DNV GL, Arnhem, The Netherlands. The OPAL-RT real-time simulator is a multipurpose platform that enables real-time simulation and rapid control prototyping. OPAL-RT is widely used in real-time analysis and control of various power-electronics applications including wind-turbine emulation [15], fuel-cell modeling [16], and analysis of smart-grid performance [17].

The primary goal of this paper is to demonstrate the use of different widebandwidth identification techniques to extract vital stability information from a microgrid. This paper will show in detail, how pseudorandom broadband injections and Fourier techniques are implemented, and how the techniques can be applied in real-time measurements. The second goal of this paper is to provide a proof-of-concept of the previously presented wideband methods by applying them in a system capable of having 200-kW power level. This paper also provides a short review of pseudorandom perturbation sequences suited for linear systems, nonlinear systems, and systems having multiple (coupled) inputs and outputs. The presented methods are highly efficient, particularly in on-board systems because the required excitation signals can be internally generated by any existing converter in the power system, and the measured frequency response (impedance/admittance/loop gain) can be rapidly extracted without an external data-acquisition unit.

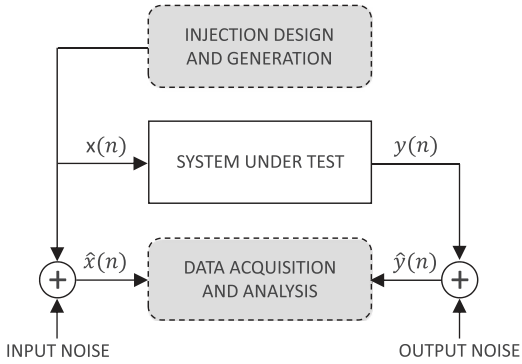

Fig. 2. Typical measurement setup.

The remainder of this paper is organized as follows. Section II reviews the theory of the wideband impedance-measurement techniques applied in this paper. Section III introduces the high-power PHIL setup recently developed at DNV GL, and provides the design steps for implementing the frequency-response measurements. Section IV presents experimental results in which all the introduced pseudorandom sequences are utilized. Finally, Section V draws the conclusion.

II. Methods

A. Frequency-Response Measurement

Fig. 2 shows a typical measurement setup where the system under test is to be identified. The system is perturbed by the excitation $x(n)$, which yields the corresponding output response $y(n)$. The measured input and output signal, $\hat{x}(n)$ and $\hat{y}(n)$, are corrupted by input noise and output noise, respectively. The noise signals are assumed to resemble white noise and are uncorrelated with $x(n)$ and $y(n)$. All of the signals are assumed to be zero mean sequences. In noisy environments, the logarithmic averaging procedure [18] is used to compute the frequency response of the system under test as

$$G_{\log}(j\omega) = \left(\prod_{k=1}^{P} \frac{\hat{Y}_k(j\omega)}{\hat{X}_k(j\omega)} \right)^{1/P} \tag{1}$$

where $\hat{X}(j\omega)$ and $\hat{Y}(j\omega)$ are Fourier-transformed input and output sequences (measured), and P denotes the number of injected excitation periods. In this method, the measurements from both input and output sides are segmented and Fourier transformed after which (1) is applied. The method tends to cancel out the effect of uncorrelated noise from both input and output sides so that the frequency response is obtained more accurately compared to conventional cross-correlation techniques [18].

The following will review three types of pseudorandom-sequence injections, which are well-suited for online frequency-response measurements of single- and multiconverter systems:

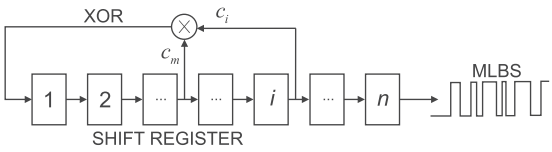

Fig. 3. *n*-bit shift register with XOR feedback for MLBS generation.

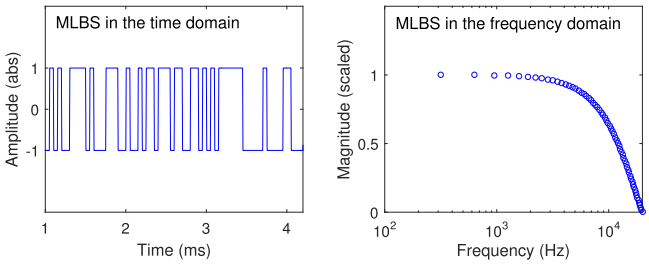

Fig. 4. MLBS injection in the time and frequency domains.

1) the conventional maximum-length binary sequence (MLBS) for linear systems;
2) periodic ternary sequences for systems exhibiting strong nonlinearities;
3) orthogonal binary sequences for systems having multiple (coupled) inputs and outputs.

B. Linear Systems: MLBS

PRBS is a periodic broadband signal based on a sequence of length N. The most commonly used pseudorandom signals are known as MLBS [19]. Such sequences exist for $N = 2^n - 1$, where n is an integer. The reason for their popularity is that they can be generated using feedback shift register circuits, as shown in Fig. 3.

Fig. 4 shows one period of a 63-b-long MLBS in the time and frequency domains. The sequence is generated at 20 kHz and has signal levels $\pm$ 1 V. The power spectrum has an envelope and drops to zero at the generation frequency.

The MLBS x has the lowest possible peak factor $|x|_{\text{peak}}/x_{\text{rms}} = 1$ regardless of its length. Hence, the sequence is well suited for sensitive systems which require small-amplitude perturbation. Due to the deterministic nature of the sequence, the signal can be repeated and injected precisely and the SNR can be increased by synchronous averaging of the response periods. Because the sequence has only two different signal levels, the signal generation can be easily embedded into a control system of any existing converter in the system.

C. Systems Exhibiting Nonlinearities: Ternary Sequence

Fig. 5 shows a conceptual diagram of a practical measurement setup in which both the linear and nonlinear components of the system under test are considered. The nonlinearities could be further separated to even- and odd-order nonlinearities [20].

Basically, a system exhibiting nonlinearities can be modeled in two ways. One method is to identify the system including all of its nonlinearities [20]. The other way is to identify only the linear portion of the model, which requires that the nonlinearities are suppressed. The latter technique is useful for power-electronics systems, where the nonlinearities are typically difficult to detect and model. In addition, usually the converter design is based on the linear model, which makes the nonlinear parts impracticable. One method of minimizing the effect of nonlinearities is to carefully select the excitation signal.

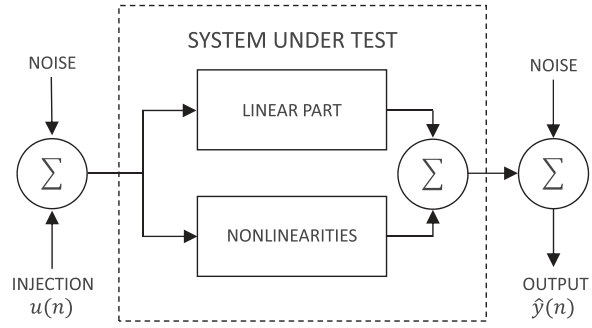

Fig. 5. Conceptual diagram of frequency-response measurement setup.

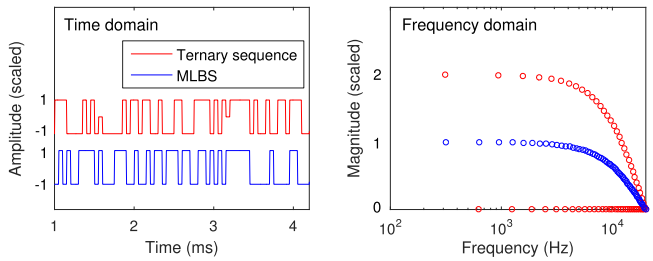

Fig. 6. Ternary sequence and MLBS in the time and frequency domains.

A ternary sequence is a broadband perturbation that has three levels and an average close to zero. The sequence can be designed to have harmonic multiples of two (2, 4, 6, ...) suppressed or harmonic multiples of two and three (2, 3, 4, 6, 8, 9, ...) suppressed [21].

The synthesis of ternary sequences has been well documented [22], [23]. All of the proposed methods aim to produce a three-level signal $u(n)$ that is inverse repeat, that is, the latter half period of the signal is negative of the first half period, defined as

$$u(n) = -u(n + N/2), 0 \leq n \leq N/2 \tag{2}$$

where N is the signal length. Because the signal is inverse repeat, it cancels out the most dominating nonlinearities from the system output, more details can be seen in [14].

In this paper, a MATLAB-based package ***prs*** is applied to design the ternary sequences [24]. The package is freely available online for generating sequences up to $N = 50\,000$. Fig. 6 shows a sample of a 64-b-length ternary sequence and a 63-b-length conventional MLBS in the time and frequency domains. The ternary sequence has values of $-1, 0$, and $+1$, and the MLBS -1 and $+1$ (the magnitude axis are scaled to facilitate the illustration). Both sequences have been generated at 20 kHz. The

power spectra of the sequences have almost identical shape, but every other harmonics of the ternary sequence has zero energy.

The ternary sequences provide good immunity against the effect of nonlinear distortions. As the harmonic multiples of two are suppressed, the sequences allow contributions of odd-order and even-order nonlinearities to be separated at the system output. Because the ternary sequences have no energy at even-harmonic components, when these sequences are used as an excitation, even-order nonlinearities in the system would result in nonzero even-harmonic components at the output, thus, giving information on the nonlinearities. Ternary sequences have been successfully applied, for example, in wireless data delivery [25], (simulated) distillation column [23], and in computer-based applications [26].

An additional advantage of the ternary sequences compared to the MLBS is that the ternary sequence can be designed for a much wider range of signal lengths. The length of a conventional MLBS is, by definition, $N = 2^k - 1$, where k is a positive integer so that $N = 3, 7, 15, 31, 63, 127, \ldots$. Thus, the sequence length must be approximately doubled each time when higher frequency resolution is required. This may quickly result in issues with computing power. As the ternary sequences exist for $2N$, they allow much more efficient optimization with respect to computing power.

D. Systems Having Multiple Inputs and Multiple Outputs: Orthogonal Binary Sequences

Most ac and dc power distribution systems are multiple-input-multiple-output (MIMO) systems. They have more than one input and output, and most often, the inputs and outputs are coupled. A good example is a multi-converter system often found in on-board applications [3]. In such systems, multiple converters are connected to the same dc bus, thus, creating a complex interconnected system. Another good example of a MIMO process is the impedance measurement in the direct-quadrature (dq) reference frame [27].

Frequency responses of MIMO systems are conventionally measured by applying the superposition theorem; a broadband excitation is injected to each system input, the responses are measured at all outputs in turn, and (1) is applied to each input and output signal combinations. A highly acceptable alternative to analyze the MIMO systems is to apply orthogonal binary sequences. In the method, several orthogonal injections are simultaneously injected (e.g., by the existing converters in a multiconverter system). As the injections are orthogonal, that is, they have energy at different frequencies, several frequency responses can be measured at the same time within one measurement cycle. The technique has several considerable advantages over the methods using sequential perturbation of the individual converters. This approach not only saves overall experimentation time, because the system has to be allowed to settle to a dynamic steady state only once, but also ensures that each frequency response is measured under same system operating conditions, which may not be the case if sequential perturbations are applied.

Previous studies have widely examined the synthesis of orthogonal injection sequences applicable to MIMO systems

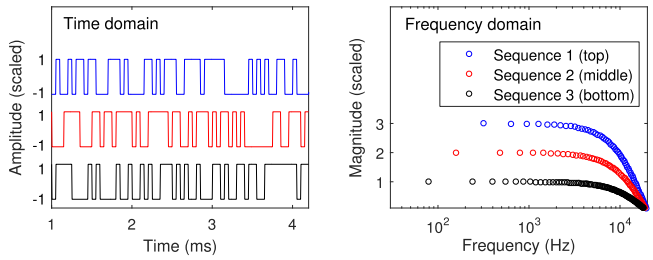

Fig. 7. Three orthogonal MLBS in the time and frequency domains.

[13], [19], [28], [29]. Two approaches for generating such sequences are commonly used. The first one applies shifted versions of the same signal to excite the various inputs, and separates their effects using cross-correlation techniques [30]. The other approach applies uncorrelated orthogonal signals so that the effects of different inputs are decoupled. The latter technique reduces the overall measurement time compared to the first approach, and also guarantees that the system operating conditions are not changed between the measurements. This paper utilizes this latter technique, using the set of orthogonal excitation sequences obtained as follows [19].

1) Generate a conventional MLBS by using a shift-register circuitry with feedback.
2) The second signal is obtained by forming an *inverse-repeat sequence* from the MLBS; that is, by adding, modulo 2, the sequence 0 1 0 1 0 1 . . . to the first sequence.
3) The third sequence is obtained by adding, modulo 2, the sequence 0 0 1 1 0 0 1 1 . . . to the original MLBS.
4) The fourth sequence is obtained by adding, modulo 2, the sequence 0 0 0 0 1 1 1 1 0 0 0 0 1 1 1 1 . . . to the original MLBS, and so on.

Fig. 7 shows samples of three orthogonal binary sequences in the time and frequency domain obtained by the presented method. The first sequence is produced by a 6-b-length shift register. All of the sequences are generated at 20 kHz. The energy values are scaled to facilitate the illustration. The three signals have nonzero energy only at different frequencies, i.e., if one signal has nonzero energy at a certain frequency, the other two signals have zero energy at that frequency. The energies of all sequences drop to zero at the generation frequency and its harmonics.

III. System Setup and Implementation

The power-hardware-in-the-loop (PHIL) setup shown in Fig. 8 at DNV GL Flexible Power Grid Lab (FPGL) is made up of 200-kVA Egston digital power amplifier, and the OPAL-RT real-time digital simulator (includes Xilinx Virtex-7 FPGA VC707). The digital power amplifier consists of four groups of four single-phase units (i.e., 16 units) with a total rated power of 200 kVA and a closed-loop bandwidth of 5 kHz. The individual digital power amplifier is realized by six interleaved parallel half-bridge converters with an equivalent switching frequency of 125 kHz. For the closed-loop PHIL setup, the high-speed SFP communication link is established between OPAL-RT and Egston. The current and voltage measurements are read back from digital amplifier output terminal

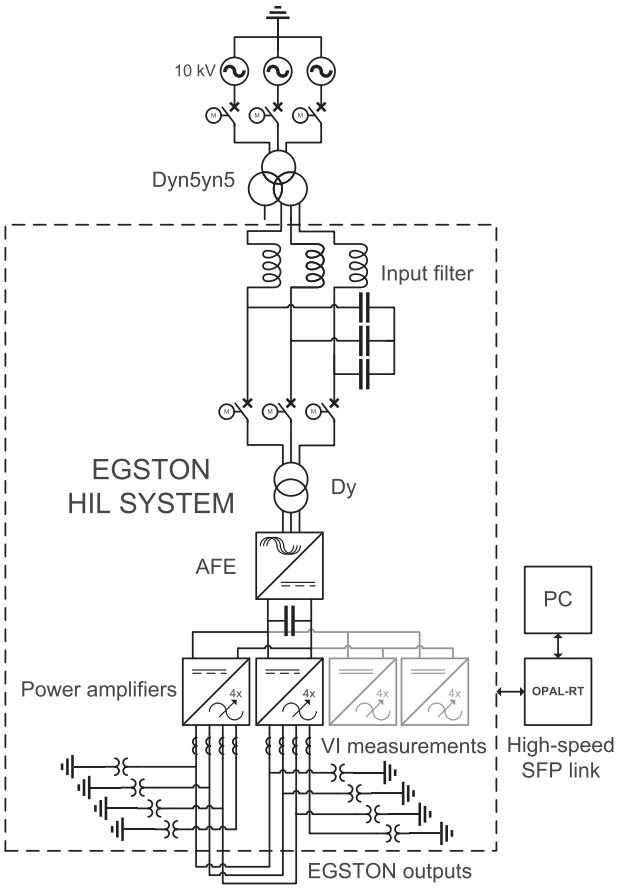

Fig. 8. PHIL setup in DNV GL Flexible Power Grid Lab.

to OPAL-RT every 4 μs, while the voltage and current control signal setpoints are sent to Egston digital I/O box. A host PC is connected via asynchronous ethernet to the OPAL-RT target PC. As shown in Fig. 8, the power amplifiers are isolated from the mains by a Dy transformer and 200-kW active front-end. The power amplifiers can be freely configured to act as sources or loads depending on what kind of power system architecture is studied. As an example, the amplifier group no. 1 on the left is configured to emulate a three-phase inverter, while the amplifier group no. 2 is configured to emulate three-phase voltage of the power system.

A. PHIL Implementation

Fig. 9 shows a diagram of the real-time spectrum analyzer implemented in OPAL-RT. The analyzer includes the injection design and synthesis, the actual injection, and data acquisition. All the rectangular (solid) boxes denote the Simulink blocks that are used for OPAL-RT. The shift register used for generating the MLBS is implemented by unit-delay blocks. The output of exclusive-or (XOR) replaces the first bit of the sequence through feedback. The generation frequency of the injection is set by the delay value of the unit-delay blocks. It should be emphasized that the selection of the feedback connections (stages) is important. Very few of the possible connections result in sequence of the maximum length of $2^n - 1$ (some sequences can be produced from several different stages). A comprehensive list of feedback connections that produce maximum-length sequences can be found, e.g., in [19]. The ternary and orthogonal sequences can be similarly synthesized by unit-delay blocks.

The designed perturbation is amplified by an adjustable gain (K). The presented concept allows continuous and repeating generation and injection of the perturbation into the system. The presented implementation also makes it possible to change the injection amplitude in real time. Hence, depending on the noise level and nonlinearities, the amplitude can be experimentally adjusted so that the produced injection energy is sufficient.

The measurements of input and output data are continuously collected and buffered. The logarithmic averaging procedure shown in (1) is applied once the data sequences have been Fourier transformed. The Bode plot is obtained by computing the magnitude and phase from the complex data. The refresh rate of the Bode plot is PN/f_g, where P is the number of injection periods, N is the injection length, and f_g is the injection generation frequency.

IV. Experiments

Three sets of experiments were performed using the PHIL setup (see Fig. 8) and the real-time spectrum analyzer (see Fig. 9). A three-phase converter, schematically shown in Fig. 10, was emulated in the setup by using two of the four power amplifiers available in the system. The emulated converter consists of Amplifier group 1, output filter, internal current control, and phase-locked loop. The filter was implemented physically using a 2-mH three-phase inductor, and the control functions were executed using the OPAL-RT.

In the first experiment, a conventional MLBS was applied, and the PLL loop gain was measured. The second experiment considered nonlinearities, and a ternary-sequence injection was applied to measure the converter output impedance. The third experiment applied orthogonal binary sequences, and the converter current loops were measured. A sine-sweep-based network analyzer was used in all experiments to obtain a reference response and compare the results. All signals were sampled at 20 kHz.

A. Experiment 1: Applying MLBS

In the first experiment, an MLBS injection was applied for measuring the PLL loop gain. The purpose of the experiment was to validate the controller of the PLL which was designed offline by using the small-signal model presented in [31]. The loop gain was designed to have a crossover frequency of 20 Hz and a phase margin of 65° for yielding sufficient transient behavior.

The MLBS for measuring the loop gain was generated at 5 kHz using a 11-b-length shift register. The MLBS was thus 2047 b long; hence, yielding a frequency resolution of approximately 4.9 Hz. The MLBS injection was placed on top of the error signal of the PLL. After this, the signals at both sides of the injection point were measured, and (1) was applied over five injection periods.Fig. 11 shows the measured loop gain of the PLL. As the figure shows, the results obtained by the MLBS accurately follow the reference. The measured loop gain validates

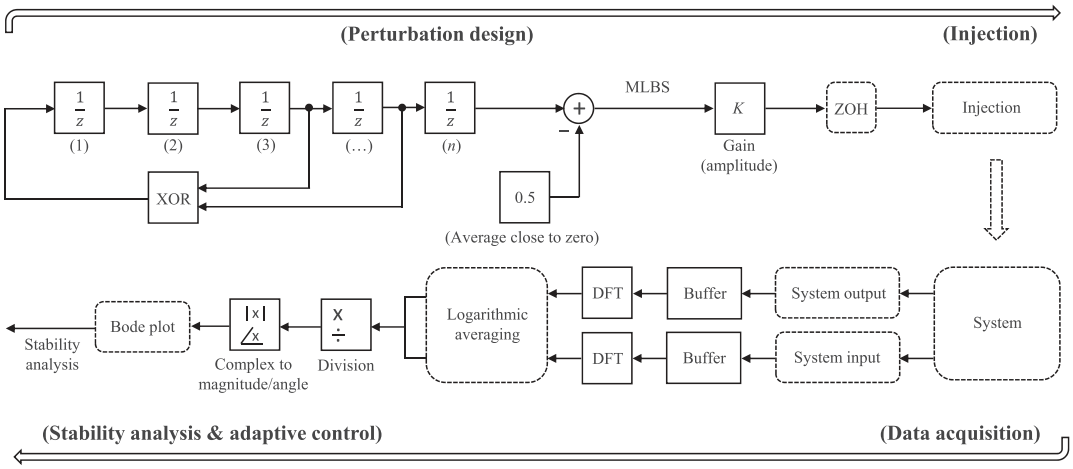

Fig. 9. Diagram of the excitation generation, injection, and data collection.

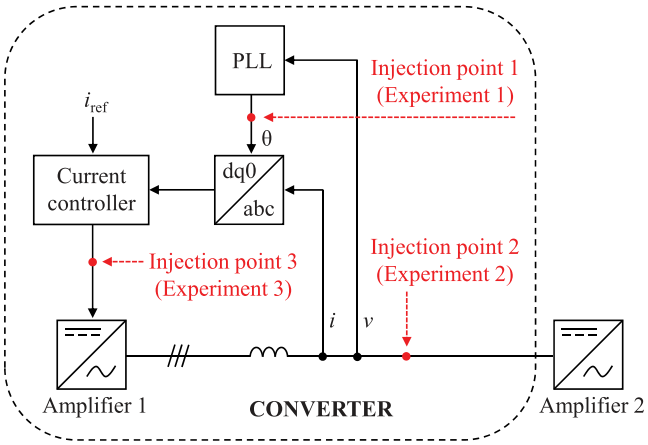

Fig. 10. Injection points of the converter under test.

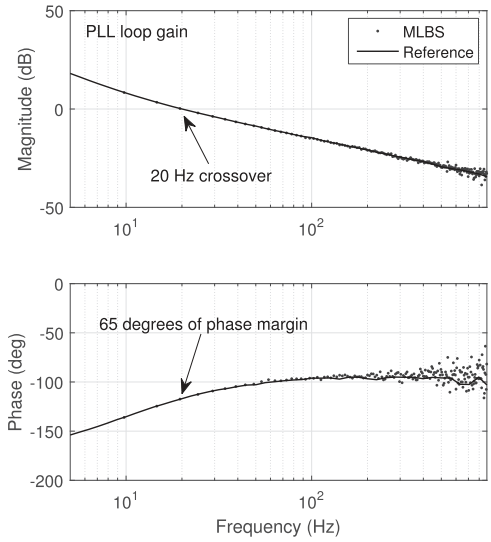

Fig. 11. Measured PLL loop gain by using conventional MLBS injection and sine sweeps (reference).

the control design. The measurement time using the MLBS was approximately 2.0 s, whereas the measurement time using the sine sweeps (reference) was several minutes.

B. Experiment 2: Applying Ternary Sequence

In the second experiment, the effectiveness of the ternary sequence is demonstrated by measuring the converter output impedance. Such measurement is important in onboard microgrids to avoid impedance-based interactions and instability between source and load converters [32].

A 2042-b-length ternary sequence with harmonic multiples of two suppressed was generated with a MATLAB-based package *prs* [24]. For comparison, a 2047-b-length MLBS was also produced. In the experiment, both sequences were generated at 5 kHz, which gave a frequency resolution of approximately 2.4 Hz. In order to increase the effect of system nonlinearities to the measured impedances, the injection amplitude was set to a very low value (0.1% of the nominal output voltage of Amplifier 2). Note that this amplitude value was unnecessarily small, but it was only used to provide a good demonstration of the potential of the ternary sequences.

Both the ternary sequence and MLBS injection were separately placed on top of the output voltage (q component) of Amplifier 2 (see Fig. 10), and the converter output voltage and current were measured. For both measurements, an averaging was applied over five injection periods; hence, the measurement time was approximately 2.0 s. The collected data were segmented, after which (1) was applied. Fig. 12 shows the converter output impedance (q component) obtained by both injections. As the figure shows, the impedance produced by the ternary sequence is accurately obtained, whereas the impedance obtained by the MLBS has relatively strong nonlinear distortions. The output impedance d component shows similar behavior.

C. Experiment 3: Applying Orthogonal Binary Sequences

The third experiment shows the application of orthogonal binary sequences. In the experiment, the converter current control loops (both d and q components) were simultaneously measured,

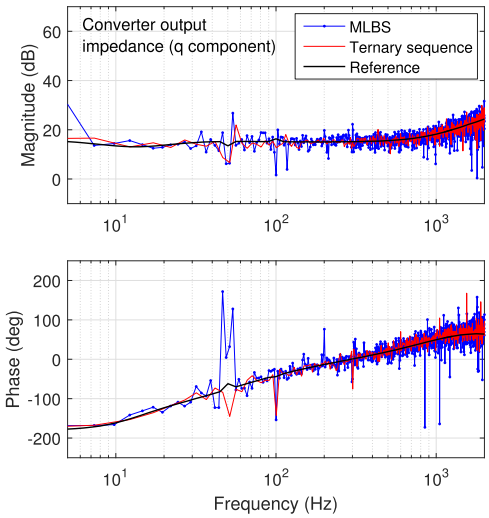

Fig. 12. Measured converter output impedance (*q* component) by using MLBS, ternary sequence, and sine sweeps (reference).

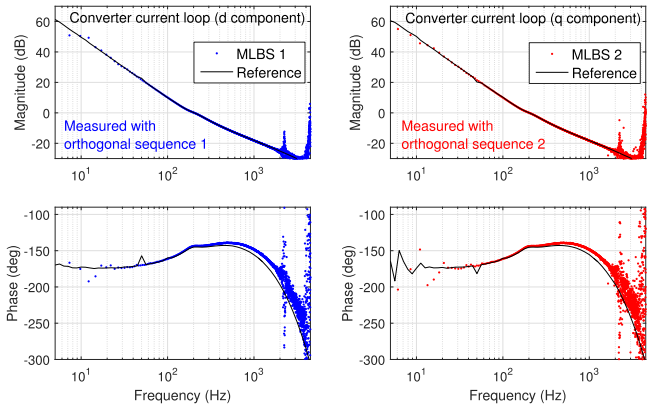

Fig. 13. Simultaneously measured *d* and *q* components of converter controller current loop using orthogonal binary sequences.

and the controller was redesigned based on these measurements. Two orthogonal binary sequences were designed using the technique shown in Section II. The first sequence was generated by a 12-b-length shift register; thus, yielding a 4095-b-long binary sequence. The second orthogonal sequence had thus, by definition, 8190 b.

Each sequence was generated at 5 kHz. The first sequence was applied with ten periods and the second sequence with five periods. Therefore, the total injection time was approximately 8 s. Both orthogonal sequences were simultaneously placed on top of the output current of the current controller; the first sequence was injected into the *d* component and the second sequence into the *q* component. After this, the signals at both sides of the injection point(s) were measured, and (1) was applied. The injection amplitudes were selected such that the perturbed control signals deviated approximately 2% from the nominal control signals.

Fig. 13 shows the measured *d* and *q* components of the controller current loop. As the figure shows, the loop gains obtained by the orthogonal sequences relatively well follow the references in a wide range of frequencies. Both components show a phase

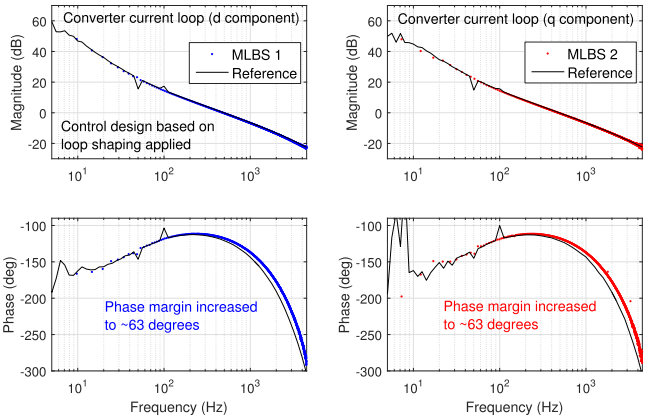

Fig. 14. Measured converter control current loop after loop shaping.

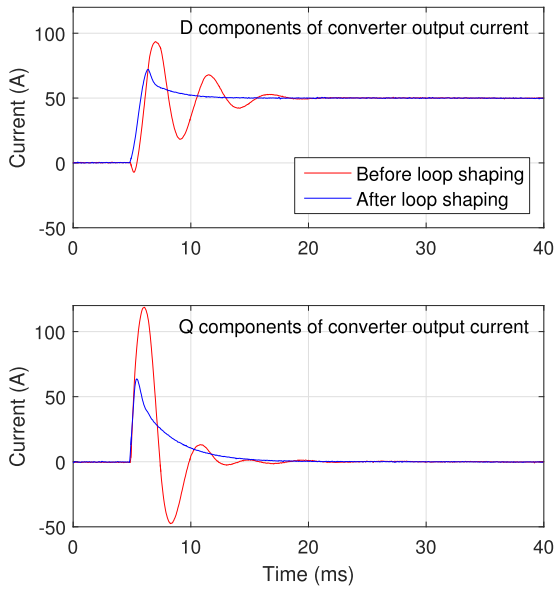

Fig. 15. Transient responses of *d* and *q* components of the converter output current.

margin of approximately 35°, thus, indicating a weak transient behavior.

The controller was redesigned based on a loop-shaping technique [33]. Fig. 14 shows the measured *d* and *q* components of the controller current loop after the control design. The phase margins of both components are now approximately 63°. The improved transient behavior of the converter output current is shown in Fig. 15.

D. Discussion

It has been shown that the proposed perturbations and signal-analysis methods can be straightforwardly designed and synthesized. However, the applicability of the proposed methods to actual on-board systems requires some considerations. First, there are several methods to implement the injection(s). The most desired method would be generating the injections by the existing converters in the system. The injection can be placed, for example, directly in the converter duty cycle. In this case, the

injection amplitude should be selected such that the converter modulator does not saturate. Another technique is to add the injection to the controller current/voltage reference. However, in this case the control bandwidth may reduce the injection energy at high frequencies. One may also apply a dual injection in which the perturbation is simultaneously added to duty cycle and current/voltage references [3]. Using the dual injection, the perturbation is not rejected by the converter control action over a wide frequency band. Another issue to be considered in actual systems is the injection amplitude(s). The amplitude needs to be high enough to provide adequate signal-to-noise ratio but low enough such that normal system operation is guaranteed during the identification. If the signal levels in the system are known, one may experimentally define the appropriate injection amplitudes. Another possibility is to define the amplitudes automatically [34]. Implementing the proposed methods into actual systems will be one of the main future research topics.

V. Conclusion

Single- and multiconverter power-electronics systems play important roles in the operation of most on-board power-distribution systems. Recent studies have presented various frequency-response-based tools with which to analyze both single- and multiconverter systems. Most often, wideband measurement techniques based on broadband perturbations and Fourier techniques have been applied to obtain the frequency response from a specific converter or a subsystem required for the analysis. This paper presented implementation techniques and a proof-of-concept of the wideband methods using power-hardware-in-the-loop measurements based on an OPAL-RT real-time simulator. The PHIL setup included several power amplifiers that can be configured to emulate on-board microgrids. This paper reviewed and applied three types of pseudorandom sequences for system analysis: a conventional MLBS for linear systems, a ternary sequence for systems exhibiting strong nonlinear distortions, and orthogonal binary sequences for analysis of multiple-input-multiple-output systems. The presented methods can be used to modify various system characteristics, such as impedance behavior and control dynamics, in real time, thereby providing means for several stability and adaptive control design tools for on-board power distribution systems.

References

[1] X. Roboam, B. Sareni, and A. Andrade, "More electricity in the air: Toward optimized electrical networks embedded in more-electrical aircraft," *IEEE Ind. Electron. Mag.*, vol. 6, no. 4, pp. 6–17, Dec. 2012.

[2] G. Buticchi, L. Costa, and M. Liserre, "Improving system efficiency for the more electric aircraft: A look at dc/dc converters for the avionic onboard dc microgrid," *IEEE Ind. Electron. Mag.*, vol. 11, no. 3, pp. 26–36, Sep. 2017.

[3] A. Riccobono *et al.*, "On the stability of shipboard DC power distribution systems—Online impedance-based methods," *IEEE Electrific. Mag.*, vol. 5, no. 3, pp. 55–67, Sep. 2017.

[4] A. Formentini, D. Dewar, P. Zanchetta, P. Wheeler, D. Boroyevich, and J.-L. Schanen, "Optimal control of three-phase embedded power grids," in *Proc. IEEE Workshop Control Modeling Power Electron.*, 2016, pp. 1–6.

[5] H. Zhang, C. Saudemont, B. Robyns, and M. Petit, "Comparison of technical features between a more electric aircraft and a hybrid electric vehicle," in *Proc. IEEE Veh. Power Propulsion Conf.*, 2008, pp. 1–6.

[6] J. Sun, "Impedance-based stability criterion for grid-connected inverters," *IEEE Trans. Power Electron.*, vol. 26, no. 11, pp. 3075–3078, Nov. 2011.

[7] A. Riccobono and E. Santi, "A novel passivity-based stability criterion (PBSC) for switching converter DC distribution systems," in *Proc. IEEE Appl. Power Electron. Conf. Expo.*, 2012, pp. 2560–2567.

[8] R. Luhtala, T. Roinila, T. Messo, T. Reinikka, J. Sihvo, and M. Vilkko, "Adaptive control of grid-connected inverters based on real-time measurements of grid impedance: Dq-domain approach," in *Proc. IEEE Energy Convers. Congr. Expo.*, 2017, pp. 69–75.

[9] T. Roinila, M. Vilkko, and J. Sun, "Broadband methods for online grid impedance measurement," in *Proc. IEEE Energy Convers. Congr. Expo.*, 2013, pp. 3003–3010.

[10] D. Martin, E. Santi, and A. Barkley, "Wide bandwidth system identification of AC system impedances by applying pertubations to an existing converter," in *Proc. IEEE Energy Convers. Congr. Expo.*, 2011, pp. 2549–2556.

[11] J. Siegers, S. Arrua, and E. Santi, "Stabilizing controller design for multi-bus MVDC distribution systems using a passivity based stability criterion and positive feed-forward control," *IEEE J. Emer. Sel. Topics Power Electron.*, vol. 5, no. 1, pp. 14–27, Mar. 2017.

[12] T. Roinila, H. Abdollahi, S. Arrua, and E. Santi, "Online measurement of bus impedance of interconnected power electronic systems: Applying orthogonal sequences," in *Proc. IEEE Energy Convers. Congr. Expo.*, 2017, pp. 5783–5788.

[13] T. Roinila, T. Messo, and E. Santi, "MIMO-identification techniques for rapid impedance-based stability assessment of three phase systems in dq domain," *IEEE Trans. Power Electron.*, vol. 33, no. 5, pp. 4015–4022, May 2018.

[14] T. Roinila and T. Messo, "Online grid-impedance measurement using ternary-sequence injection," *IEEE Trans. Ind. Appl.*, to be published, 2018, doi: 10.1109/TIA.2018.2825938.

[15] A. Merabet, K. Tawfique, M. Islam, S. Enebeli, and R. Beguenane, "Wind turbine emulator using OPAL-RT real-time HIL/RCP laboratory," in *Proc. Int. Conf. Microelectron.*, 2014, pp. 192–195.

[16] E. Breaz, F. Gao, D. Paire, and R. Tirnovan, "Fuel cell modeling with dSPACE and OPAL-RT real time platforms," in *Proc. IEEE Transp. Electrific. Conf. Expo.*, 2014, pp. 1–6.

[17] D. Bian, M. Kuzlu, M. Pipattanasomporn, S. Rahman, and Y. Wu, "Real-time co-simulation platform using OPAL-RT and OPNET for analyzing smart grid performance," in *Proc. IEEE Power Energy Soc. Gen. Meeting*, 2015, pp. 1–5.

[18] R. Pintelon and J. Schoukens, *System Identification—A Frequency Domain Approach*. New York, NY, USA: IEEE, 2001.

[19] K. Godfrey, *Perturbation Signals for System Identification*. Englewood Cliffs, NJ, USA: Prentice-Hall, 1993.

[20] O. Nelles, *Nonlinear System Identification*. Berlin, Germany: Springer-Verlag, 2001.

[21] M. Foo, A. Tan, and K. Basu, "Maximum length ternary signal design based on Nyquist point mapping," in *Proc. IFAC Symp. Syst. Identification*, 2006, pp. 1127–1132.

[22] H. Barker, A. Tan, and K. Godfrey, "Ternary input signal design for system identification," *IET Control Theory Appl.*, vol. 1, pp. 1224–1233, 2007.

[23] A. Tan, K. Godfrey, and H. Barker, "Design of ternary signals for MIMO identification in the presence of noise and nonlinear distortion," *IEEE Trans. Control Syst. Technol.*, vol. 17, no. 4, pp. 926–933, Jul. 2009.

[24] A. Tan and K. Godfrey, "The generation of binary and near-binary pseudo-random signals: An overview," *IEEE Trans. Instrum. Meas.*, vol. 51, no. 4, pp. 583–588, 2002. [Online]. Available: http://www.eng.warwick.ac.uk/eed/dsm/prs

[25] Y. Ng, A. Tan, and T. Chuang, "Channel identification of concatenated fiber-wireless uplink using ternary signals," *IEEE Trans. Veh. Technol.*, vol. 60, no. 7, pp. 3207–3217, Sep. 2011.

[26] A. Angelis, J. Schoukens, K. Godfrey, and P. Carbone, "Practical issues in the synthesis of ternary sequences," *IEEE Trans. Instrum. Meas.*, vol. 66, no. 2, pp. 212–222, Feb. 2017.

[27] T. Roinila, T. Messo, T. Suntio, and M. Vilkko, "Pseudo-random sequences in DQ-domain analysis of feedforward control in grid-connected inverters," in *Proc. 17th IFAC Symp. Syst. Identification*, 2015, pp. 1301–1306.

[28] R. Luhtala, T. Roinila, and T. Messo, "Implementation of real-time impedance-based stability assessment of grid-connected systems using MIMO-identification techniques," *IEEE Trans. Ind. Appl.*, to be published, doi: 10.1109/TIA.2018.2826998.

[29] T. Roinila, H. Abdollahi, S. Arrua, and E. Santi, "Real-time stability analysis and control of multi-converter systems by using MIMO-identification techniques," *IEEE Trans. Power Electron.*, to be published, doi: 10.1109/TPEL.2018.2856532.

[30] L. Yao, J. Zhao, and J. Qian, "An improved pseudo-random binary sequence design for multivariable system identification," in *Proc. IEEE World Congr. Intell. Control Autom.*, 2006, pp. 1768–1772.
[31] T. Messo, J. Jokipii, A. Mäkinen, and T. Suntio, "Modeling the grid synchronization induced negative-resistor-like behavior in the output impedance of a three-phase photovoltaic inverter," in *Proc. IEEE Int. Symp. Power Electron. Distrib. Gener. Syst.*, 2013, pp. 1–7.
[32] B. Wen, R. Burgos, D. Boroyevich, P. Mattavelli, and Z. Shen, "AC stability analysis and dq frame impedance specifications in power electronics based distributed power systems," *IEEE J. Emerg. Sel. Topics Power Electronics*, vol. 5, no. 4, pp. 1455–1465, Dec. 2017.
[33] T. Suntio, T. Messo, and J. Puukko, *Power Electronic Converters: Dynamics and Control in Conventional and Renewable Energy Applications*. Weinheim, Germany: Wiley-VCH, 2017.
[34] M. Shirazi, J. Morroni, A. Dolgov, and D. Maksimovic, "Integration of frequency response measurement capabilities in digital controllers for DC-DC converters," *IEEE Trans. Power Electron.*, vol. 23, no. 5, pp. 2524–2535, Sep. 2008.

Tomi Roinila (M'10) received the M.Sc. (Tech.) and Dr.Tech. degrees in automation and control engineering from Tampere University of Technology (TUT), Tampere, Finland, in 2006 and 2010, respectively.

He is currently an Academy Research Fellow with TUT. His main research interests include modeling and control of grid-connected power-electronics systems, and modeling of multiconverter systems.

Tuomas Messo (M'14) received the Dr.Tech. degree in electrical engineering from Tampere University of Technology, Tampere, Finland, in 2014.

Since 2016, he has been working as an Assistant Professor with Tampere University of Technology, Laboratory of Electrical Energy Engineering in the field of power electronics. His research interests include grid-connected three-phase power converters for renewable energy applications and microgrids, dynamic modeling, control design, impedance-based interactions in three-phase systems and impedance design of grid-connected inverters.

Roni Luhtala (S'17) received the M.Sc. degree in automation and control engineering from Tampere University of Technology (TUT), Tampere, Finland, in 2017. Since 2017, he has been working as a doctoral student with the Laboratory of Automation and Hydraulics, TUT.

His main research interests include real-time impedance identifications and adaptive control of grid-connected inverters.

Rick Scharrenberg was born in the Netherlands in 1992. He received the B.Sc. degree in electrical engineering from Eindhoven University of Technology, Eindhoven, The Netherlands, in 2014.

During the last year of his master program, he completed his graduation project about HVdc Protection Systems, Transmission and Distribution Systems Center, Mitsubishi Electric Corporation, Kobe/Itami, Japan. In 2015, he started working as a Consultant within the New Energy Technologies Team, DNV GL in Arnhem, where he was involved in energy storage projects. Since 2017, he is working as an Innovation Engineer with the KEMA Laboratories within the same company, where he is mainly involved in the testing of power-electronics based systems, such as PV inverters, battery converters, and energy storage systems. His research interests include power electronics, energy storage, renewable energy, and HVdc.

Erik C. W. de Jong (M'05–SM'12) received the B.Ing. (*cum laude*) and M.Ing. (*cum laude*) degrees in electric and electronic engineering from the Rand Afrikaans University, Johannesburg, South Africa, in 2001 and 2003, respectively, and the Ph.D. degree in electrical engineering from Delft University of Technology, Delft, The Netherlands, in 2007.

Since 2007, he has been with DNV GL/Energy, Arnhem, The Netherlands, as a technical professional, specializing and providing consultancy services in power electronics and its applications in utility grids. Since 2008, he has been also with the Flex Power Grid Laboratory as a General Manager responsible for all operations regarding medium-voltage grid inverter research, testing, and certification. In 2010, he received the prestigious Hidde Nijland Award for his contributions in the field of testing utility-interactive power electronics. Since 2013, he is also a Senior Researcher in the field of power electronics and power cybernetics with DNV GLs Strategic Research and Innovation Department. He serves as an Expert in the IEC 61400-21 Standardisation Maintenance Team (TC88) for revision 3 on Power Quality, industry member of the DERLab Association, and the Dutch delegate for the Smart Grid International Research Facility Network activities. As a part-time Associate Professor at the Technical University of Eindhoven, Electrical Energy Systems Group, he directs research programs and guides Ph.D. students in the field of power electronics dominated (smart) grids. He is very active in publishing scientific research results in peer reviewed international conferences and journals.

Alejandra Fabian received the B.Sc. degree in electronics technology from Monterrey Institute of Technology and Higher Education, Estado de Mexico, Mexico, in 2011, and the M.Sc. degree in sustainable energy technology from Eindhoven University of Technology, Eindhoven, The Netherlands, in 2016.

She is currently a Researcher with DNV GL Group Technology and Research, Arnhem, The Netherlands. Her research interests include hardware in the loop methods, power systems, and control applications for renewable energy integration.

Yin Sun received the M.Sc. degree in sustainable energy technology from the University of Twente, Enschede, Netherlands, in 2010. Since 2014, he has been a part-time Ph.D. student with Electrical Energy System Group, Eindhoven University of Technology, Eindhoven, The Netherlands.

He is currently a Senior Researcher at DNV GL Group Technology Research, Arnhem, The Netherlands. He has been working with KEMA (predecessor of DNV GL) since 2010 as a power system analysis consultant in the power grid design/analysis, engineering, and commissioning support. His research topic focuses on the stability of power electronics dominant grid, especially the harmonic stability induced by complex converter control interaction. He is also a technical expert in the CIGRE C4. B4. JWG38 (Network Harmonic Calculation) and IEC SC8A (renewable grid compliance).